β^+ decay of ^{61}Ga

L. Weissman,[1,*] J. Cederkall,[1] J. Äystö,[1,2] H. Fynbo,[1] L. Fraile,[1] V. Fedosseyev,[1] S. Franchoo,[1] A. Jokinen,[1,2] U. Köster,[1] G. Martínez-Pinedo,[3] T. Nilsson,[1] M. Oinonen,[1,4] K. Peräjärvi,[1,5] M. D. Seliverstov,[6] and ISOLDE Collaboration

[1]*CERN, EP-Division, CH-1211, Geneve 23, Switzerland*

[2]*Department of Physics, University of Jyväskylä, FIN-40100, Jyväskylä, Finland*

[3]*Department für Physik und Astronomie, Universität Basel, CH-4056 Basel, Switzerland*

[4]*Helsinki Institute of Physics, FIN-00014, Helsinki, Finland*

[5]*Johannes-Gutenberg-Universität, Institut für Physik-EXAKT, D-55099 Mainz, Germany*

[6]*Petersburg Nuclear Physics Institute, 188350, Gatchina, St.-Petersburg, Russia*

(Received 10 December 2001; published 29 March 2002)

The mirror β^+ decay of ^{61}Ga was investigated by means of β- and γ-ray spectrometry at the ISOLDE-PSB facility using laser ionization and mass separation. The results for the ^{61}Ga half-life and the Q_{EC} value are 168(3) ms and 9255(50) keV, respectively. The β-decay strength to the ground and low-lying excited states of the daughter ^{61}Zn was deduced. The experimental results are in a good agreement with large-scale shell-model calculations.

DOI: 10.1103/PhysRevC.65.044321 PACS number(s): 32.80.Fb, 27.50.+e

I. INTRODUCTION

According to the experimentally proved conserved vector current (CVC) hypothesis the Fermi (F) β decay is expected to have a constant strength for analog transitions for a given isospin multiplet, independent of the nuclear structure. The situation is quite different for the Gamow-Teller strength $B(\mathrm{GT})$, which depends on a product of the GT-matrix element $\langle \sigma\tau \rangle$ and the axial-vector constant g_a. The presence of the nuclear environment results in renormalization of the free-nucleon g_a axial-vector constant, determined by the neutron β decay. The GT-matrix element also varies from nucleus to nucleus. It is thus a challenge to calculate the strengths for the GT transitions with the same high accuracy as of for the F decay [1], as well as to disentangle the matrix element from the axial-vector constant from the experimentally measured $B(\mathrm{GT})$. The measurement of β decays of $T=1/2$ mirror nuclei, characterized by a mixture of fast F and allowed GT transitions, gives a unique opportunity to study the Gamow-Teller β decay between isobaric analog states.

Since the strength of the F transitions is constant for mirror transitions, the $B(\mathrm{GT})$ strength can be evaluated very accurately and compared with theoretical calculations. The similarity of the wave functions for members of mirror doublets simplify theoretical calculations. Studies of mirror nuclei can therefore be used to test various theoretical models related to, e.g., spin-isospin excitation modes. Moreover, the accurate measurements of the β-decay strength and the magnetic moments of the mirror states would allow one to evaluate the effective axial-vector constant in a given nucleus [2].

In this context the expansion of our knowledge of mirror decays for the heaviest available mirror nuclei in the *fp* shell is of significant importance. These studies are also becoming increasingly important in the context of recent progress in large-scale shell-model calculations, which at present are extended up to the $A=65$ mass region [3,4]. The GT-matrix elements of mirror decays have been measured with high accuracy in the *fp* shell from ^{41}Sc up to ^{55}Ni [5–12]. Information on the GT strength was obtained for heavier nuclei in the *fp* shell [13–16]. This paper reports on a new measurement of the mirror β^+ decay of the ^{61}Ga nucleus ($Z=31, N=30$).

Excited levels of the daughter nucleus ^{61}Zn are well known from reaction studies [17,18] and in-beam spectroscopy experiments [19–22]. The half-life of ^{61}Ga, produced in fragmentation reactions, was measured with 20% accuracy by Winger *et al.* [23]. The first spectroscopic details of the ^{61}Ga β^+ decay were later obtained at the GSI On-Line Mass Separator [14]. However, as a result of the lack of chemical selectivity, that experiment suffered from strong ^{61}Zn and ^{61}Cu isobaric contaminations, resulting in a limited accuracy for the measurement. The present study used resonance laser ionization of Ga inside the ion source combined with on-line mass separation at the ISOLDE high-resolution mass separator (HRS).

II. EXPERIMENT

Neutron-deficient gallium isotopes were produced in spallation reactions induced by a pulsed beam of 1.4 GeV protons with an average proton current of 2 μA coming from the CERN PS-Booster and impinging on a zirconium oxide target (8 g/cm^2 of Zr). The reaction products diffuse from the heated target chamber ($T \approx 1850\,^\circ$C) and are guided to a niobium ionizer tube. Ionization of Ga atoms was performed using the Resonance Ionization Laser Ion Source (RILIS) described in Refs. [24,25]. A two-step ionization scheme used for the production of gallium ions [26] was applied. In this scheme an atom is excited from the $4s^2 4p^2 P_{1/2}$ ground state to the $4s^2 4d^2 D_{3/2}$ (287.42 nm) excited state following a second excitation step to the continuum. The first excitation step was provided by a tunable pulsed dye laser, where the

*Corresponding author. Present address: NSCL, Michigan State University, East Lansing, MI 48824. Electronic address: weissman@nscl.msu.edu

required ultraviolet radiation was created by frequency doubling in a nonlinear BBO crystal. Pumping of the dye lasers and the final second excitation step was obtained by copper vapor lasers with wavelengths of 511 nm and 578 nm, operating at a pulse repetition rate of 11 kHz. The laser beams shine into the ion-source cavity, which consists of a tungsten tube of 30 mm length and 3 mm inner diameter. The average laser beam power delivered to the ion source was 100 mW and 8 W for the first and second steps, respectively. The efficiency of ionization for Ga was measured in previous off-line experiments, reaching a maximum value of 21%. Since the ionization threshold for Ga atoms is relatively low (6.11 eV), thermal ionization of gallium takes place as well in a hot cavity. The selectivity of the RILIS is consequently defined as the ratio of laser-ionized to thermally ionized atoms. During the run the selectivity varied from 10 to 20.

After leaving the ion-source cavity the ions are accelerated by a 60 kV voltage and mass separated using the HRS, which has a typical mass-resolution of 5000. The mass separated ions were implanted into a movable tape in order to remove long-lived daughter activities (^{61}Zn, $T_{1/2}=1.5$ min and ^{61}Cu, $T_{1/2}=3.4$ h). The tape was moved every 7 s. The implantation chamber and detector setup were similar to those described in Ref. [27]. The implantation point was surrounded by 125 μm Kapton windows transparent to high-energy β particles. Four 1.5-mm-thick plastic detectors were positioned close to the Kapton windows for detection of β particles. The scintillation light from the plastic detectors was guided using optical fibers to two photomultipliers per detector. The signals from the photomultipliers were amplified and fast time signals generated. Only coincidences between time signals from two photomultipliers of the same detector were considered as a true detection of a β particle. This allows for an almost complete reduction of random electronic noise and provides a high detection efficiency. Two Ge detectors of 75% and 50% relative efficiency were also positioned in close geometry around the implantation point. The signals were digitized and data collected by a VME-based data acquisition system (DAQ). The efficiency of the β and γ detectors was measured using ^{49}Cr, ^{36}K, ^{50}Mn, ^{64}Ga, and ^{80}Rb sources collected on line, corresponding to a broad energy range of emitted β and γ rays. The β-detector efficiency was measured by comparing singles and β-gated Ge-detector spectra and was found to be 32(3)%. It is of special importance that the on-line sources had the same geometry as the investigated ^{61}Ga source and that all the used on-line sources were positron emitters; thus, the measured γ efficiency is effected by the summing with the 511 keV annihilation γ ray in the same way. The intensity of the on-line sources was kept low to avoid dead-time effects. The beam gate had a duration of 150 ms, with a delay of 5 ms after the proton pulse impact on the target. The measured yield of ^{61}Ga was of the order of 10 ions/μC (50 ions per a proton pulse) corresponding to about 15 counts in the β detectors per proton pulse. Even without laser ionization the spectrum was dominated by radiation from ^{61}Ga. This is due to the low ionization potential for Ga as compared to Cu and Zn, the beam gate being optimized on the release and half-life of ^{61}Ga and the efficient removal of long-lived activity by the tape-transport system.

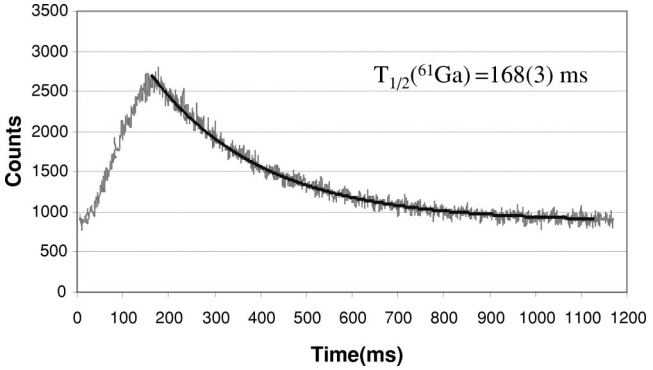

FIG. 1. Time spectrum for the β-detector trigger. The exponential fit of the decay is also shown.

III. RESULTS

The pure ^{61}Ga beam consequently allowed for an accurate measurement of the half-life. The time spectrum of the β detectors is shown in Fig. 1. The spectrum was collected during 12 h using a time stamp module measuring the delay time between the proton-pulse impact and the arrival of a trigger signal in the DAQ. In Fig. 1, one can observe the 150 ms implantation time and the following decay. A small fraction of ions was implanted next to the tape and was not removed. This background from the nonremoved daughter activity is basically constant on the time scale presented in Fig. 1 [$T_{1/2}(^{61}\mathrm{Zn})=1.5$ min]. The decay part of the time spectrum can thus be fitted with a simple exponential and a constant background term. The fit results in a ^{61}Ga half-life of 168(3) ms. The β-gated γ spectrum is shown in Fig. 2. The spectrum corresponds to a prompt time window of 600 ms after a proton pulse. The delayed background, for events occurring later than 1 s after proton pulse, was subtracted from the prompt spectrum. The background subtraction was adjusted in order to compensate for the 475 keV ^{61}Zn transition. In this way the subtraction also clears the 756 keV

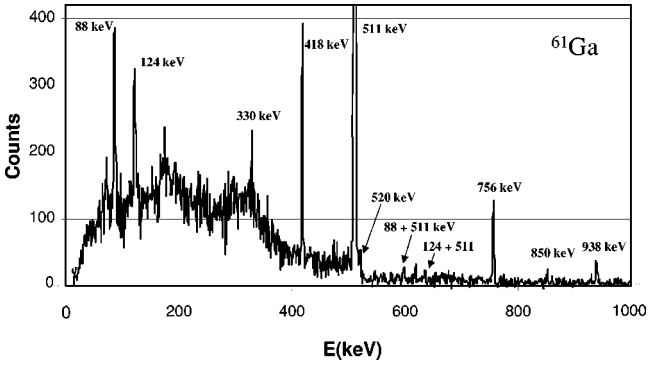

FIG. 2. β-gated Ge spectrum corresponding to a prompt time window less than 600 ms after proton-pulse impact under the condition of anticoincidence with an adjacent β detector. The background corresponding to a time window starting after 1 s was subtracted. The β^+-delayed γ transitions of ^{61}Ga are indicated.

TABLE I. The relative intensities of the investigated γ rays. The results from the previous study are also presented [14].

E_γ (keV)	Rel. int. (this experiment)	Rel. intensity ([14])
88	1.00±0.16	1.00±0.28
124	0.62±0.11	0.48±0.12
295.5	⩽0.02	
330	0.04±0.01	
337.5	⩽0.02	
418	0.72±0.12	0.40±0.06
520	0.09±0.02	
633	⩽0.01	
756	0.44±0.08	0.32±0.05
850	0.06±0.02	
938	0.21±0.04	⩽0.04
1362	⩽0.005	⩽0.05

peak from a weak contamination of the 752 keV ^{61}Zn transition. The spectrum was taken under the condition that no β particle be detected in one of the β detectors adjacent to a Ge detector, thus avoiding the possibility of β-γ summing. Some of the γ transitions in Fig. 2 are observed for the first time in ^{61}Ga β^+ decay, although all of them have been reported in in-beam experiments [19–22]. None of these transitions were observed in the background spectrum given by the delayed time window. Some weaker transitions (the 295, 337, 632, and 1362 keV transitions), which according to in-beam spectroscopy studies [19,20] are expected in the β^+-delayed γ spectrum of ^{61}Ga, were not observed. Neither were observed the γ rays from the excited levels of ^{60}Cu, indicating a rather low β-delayed proton emission probability. A summary for the relative intensities of the studied γ transition is presented in Table I together with results from the previous experiment [14].

A special effort was made to measure the Q_{EC} value. A separate detector setup was used for this measurement. The ions were similarly implanted into a movable tape. A 500 μm Si detector and a 20-mm-thick low-energy Ge detector (LEGe) were positioned in close geometry surrounding the implantation point, inside and respectively outside of the vacuum chamber. The energy spectrum of the LEGe detector was collected under the condition of coincidence between the Si and LEGe detector. The β^+-decay scheme and the Q_{EC} of ^{61}Ga are expected to be close to those of ^{62}Ga. On the other hand, the production rate of ^{62}Ga ($\approx$1000 at/μC) is two orders of magnitude higher than that of ^{61}Ga. It is thus attractive to use the positron energy spectrum from the ^{62}Ga decay as a reference for the ^{61}Ga decay. The corresponding energy spectra of ^{62}Ga and ^{61}Ga are presented in Figs. 3(a) and 3(b). They were collected during 2 and 12 h, respectively. The spectra were measured for the prompt events within 600 ms after a proton pulse, and the delayed background window was subtracted the same way as described above. The summing of positrons and 511 keV γ rays in the LEGe detector is the same for the ^{62}Ga and ^{61}Ga sources. The slight difference in the spectra may arise from the summing of positrons and the γ rays from the weakly

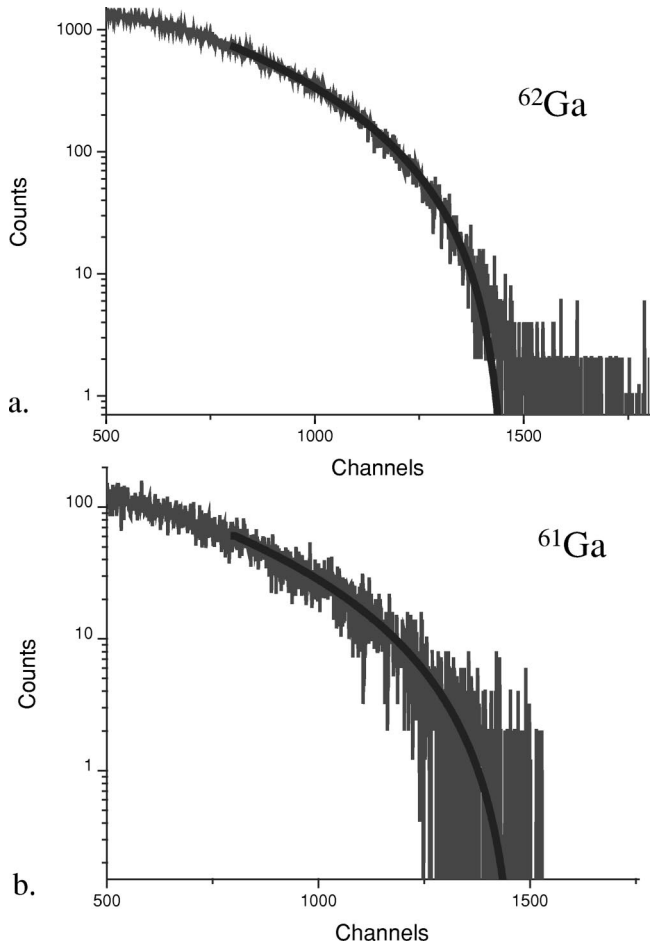

FIG. 3. The high-energy part of the positron spectra for ^{62}Ga(a) and ^{61}Ga(b) measured with the LEGe detector, under the condition of coincidence with the Si detector and applying a prompt time window. The background corresponding to the delayed time window (see text) is subtracted. The analysis of the spectrum is similar to that of Ref. [28]. The fitted functions are shown only in the selected range.

populated excited levels of ^{61}Zn. Taking the measured branching ratios to the excited levels of ^{61}Zn (Fig. 4) and estimating the total γ-detection efficiency of the LEGe detector as the detector's solid angle from the implantation point the probability of such summing can be evaluated as less than 0.5%. Moreover, the end point of the positron spectra should not change due to such summing, since the lower maximal energy of a positron decaying to an excited level is exactly compensated for by the corresponding fully absorbed γ ray. More problematic is the summing of radiation from different decays. However, since the counting rate was low for both cases, such summing is negligible.

Therefore the ^{62}Ga energy spectrum can be safely taken as a reference for ^{61}Ga. Its high-energy part was fitted to the four-parameter expression [28]

$$S(x)=N_0(a+bx+x^2)(x-x_0)^2,$$

where N_0 is an overall normalization, x is the channel number, and a, b, and x_0 (end point) are three unknown param-

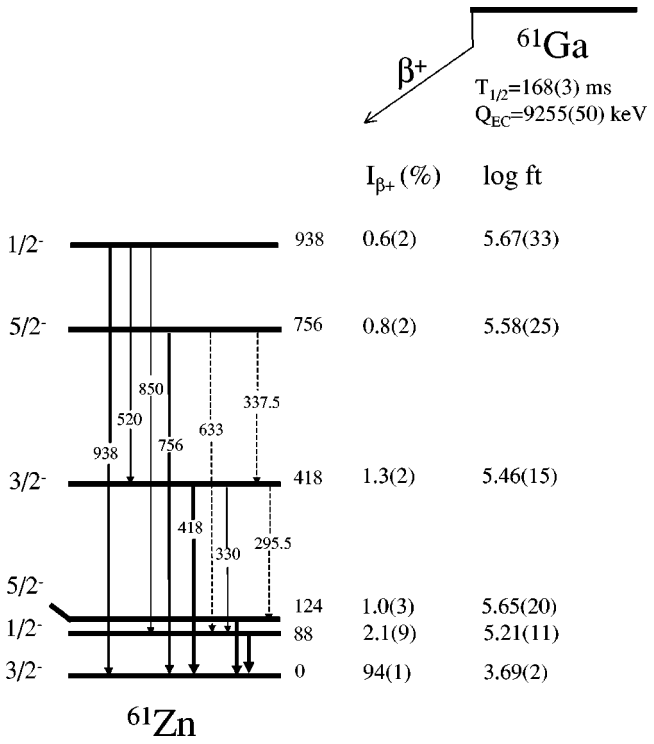

FIG. 4. The β^+-decay scheme of ^{61}Ga. Nonobserved transitions are shown with dashed lines. The larger errors for the branching ratios to the 88 keV and 124 keV levels are associated with the uncertain multipolarity of the corresponding transitions.

eters. Once a, b, and x_0 were determined for ^{62}Ga, they were fixed for fitting the ^{61}Ga spectrum. The latter was fitted by a $nS(\alpha x)$ function, where n is an overall normalization and α is a stretching factor. The fitting range was ''stretched'' by the same α factor. As a result of this procedure the end point of ^{61}Ga is determined with respect to the one of ^{62}Ga [$Q_{EC}=9171(26)$ keV [28]]. The use of ^{62}Ga as reference permits avoiding various systematic errors associated with the energy loss of the positrons during passage of the tape, the Si detector, the window of the vacuum chamber, and the dead layer of the LEGe, as well as summing effects with the 511 keV γ ray. The LEGe energy spectrum was calibrated with various on-line γ sources up to 3795.1 keV (^{64}Ga). The end points of positron spectra of various on-line sources up to 12865 keV (^{20}Na) were used to verify the general linearity of the energy spectra up to very high energy. However, the end points were not used for energy calibration due to uncertainties in energy losses and summing effects. The result of Q_{EC} for ^{61}Ga is 9255(50) keV. The main errors in this measurement are the error in $Q_{EC}(^{62}\mathrm{Ga})$, the fit error, and the uncertainty due to the slight variation of the fit result with the fitting range. It was checked that the introduction of weak decay branches to the excited levels into the fitting function do not change the result of the fitting within the fit errors.

IV. DISCUSSION

The decay and level scheme for the ^{61}Ga β^+ decay are presented in Fig. 4. The decay is dominated by a combined fast mixed F-GT transition to the ground state of ^{61}Zn. All other weak feedings to excited levels of ^{61}Zn correspond to allowed GT transitions. The relative intensities of the nonobserved weak 295.5, 633, and 337.5 keV transitions, known from [19,21], were taken into account for calculating the β-decay branching ratios. The main errors in the branching ratios of decay to the excited levels are due to the poor statistics in some γ lines and the uncertainty in the detector efficiency. Special consideration is needed for the low-energy 88 keV and 124 keV transitions (see Table II). In Ref. [19] the angular distribution coefficient A_2 for the 88 keV γ ray was found to be -0.03. This A_2 value corresponds to an $E2/M1$ mixing ratio of either 0.2 or 3.8 [29]. In the first case the 88 keV transition is dominantly magnetic dipole and has an internal conversion coefficient of ≈ 0.1; the second case corresponds to a dominantly electric quadruple transition and a high internal electron conversion coefficient of ≈ 0.9. The corrected branching ratios for the decay to the 88 keV level can be either 1.5% or 2.7% depending on the multipolarity. Note that according to the systematics of fp-shell mirror nuclei, the feeding to the first excited level is always slightly stronger than the branching ratios to the higher excited levels. Therefore the 2.7% value for the branching ratio may be assigned tentatively. A similar consideration can be applied to the 124 keV transition. However, the higher energy of this transition makes the correction for internal conversion less important. In spite of the significant errors in the branching ratio into excited levels, the ground-state feeding is determined quite accurately since the feeding to all other levels is rather weak. The main error in the ground-state feeding comes from the uncertainty in the correction for internal conversion of the 88 keV transition. The nonobservation of the 1362 keV γ ray indicates that a $(3/2^-,5/2^-)$ assignment of the 1362 keV level [21], resulting in an allowed β^+ decay to this level, is probably not correct. Furthermore, nonobservation of the 61 keV transition from the ^{60}Cu 2^+ excited level in the γ spectra gives an upper limit for the proton emission probability of 0.25%.

The value obtained for the half-life is in a good agreement with two previous measurements [14,23]. The new result for Q_{EC} provides a significant improvement for the extrapolated value of 8995(196) keV [30] and is in good agreement with the results of theoretical calculations, which give 9220 [31], 9262(50) [32], and 9330 keV [33].

The obtained values of the ^{61}Ga half-life and Q_{EC} are important for further improvement of the modeling of the astrophysical rp process [41]. In particular, based on the measured Q_{EC} value of ^{61}Ga and the known masses of ^{61}Zn and ^{60}Zn [30] the proton separation energy $S_p(^{61}\mathrm{Ga})$ can be estimated as 193(55) keV. This value is somewhat smaller than the S_p from the recent mass evaluation, 454(196) keV [30], leading to a higher proton-capture cross section on ^{60}Zn, i.e., reducing the stellar half-life of this possible waiting point nucleus (see discussion in Ref. [42]).

The GT-decay strength $B(\mathrm{GT})$ can be calculated for allowed transitions from the measured ft value via the well-known formula

TABLE II. Branching ratios, logft values, and the corresponding GT strength for the ^{61}Ga β^+ decay. The presented values for the 88 keV and 124 keV levels are averaged over two possible multipolarites of the corresponding transitions (see discussion).

I^π	E_{expt} (keV)	$I_{\beta^+ expt}$ (%)	logft_{expt}	$B(\mathrm{GT})_{expt}$	E_{theor} (keV)	$B(\mathrm{GT})_{theor}$
$3/2^-$	0	94(1)	3.69(2)	0.28(7)	420.2	0.35
$1/2^-$	88	2.1(9)	5.21(11)	0.04(1)	251.9	0.0068
$5/2^-$	124	1.0(3)	5.65(20)	0.02(1)	0	0.0012
$3/2^-$	418	1.3(2)	5.46(15)	0.02(1)	706.5	0.0034
$5/2^-$	756	0.8(2)	5.58(25)	0.02(1)	1352.6	0.00033
$1/2^-$	938	0.6(2)	5.67(33)	0.02(1)	1245.1	0.18

$$B(\mathrm{GT}) = \frac{C}{(f^+ t + f^{EC} t)(1+\delta_r)} - B(F)(1-\delta_c),$$

where $C = 6145(4)$ s, $(1-\delta_C)$ is the correction for isospin impurity taken as 0.997(3), and $(1+\delta_r)$ is a radiative correction equal to 1.026 [34]. The values of the Fermi integral for the positron decay f^+ were obtained by averaging results of the calculations based on Refs. [35,36]. The f^{EC} values for the competing electron-capture process can be neglected in further considerations. Using $B(\mathrm{F}) = 1$ for the mirror transition and $B(\mathrm{F}) = 0$ for allowed GT transitions, the $B(\mathrm{GT})$ strengths are readily calculated.

The results for all observed values are presented in Table II together with the measured branching ratios and logft values. They are compared with the predictions of large-scale shell-model calculations obtained using the code ANTOINE [37] and the effective interaction KB3G [38]. The full fp shell was used as a valence space with a maximum of four nucleons being excited from the $f_{7/2}$ orbit to the rest of the shell. This model space includes 52 463 690 slater determinants. The calculations use a value of the axial-vector coupling constant, $g_A = -1.2670(35)$ [39], and a quenching factor of 0.74 [40]. The presented results are in agreement with the allowed character of a mirror transition and similar to the decay of other mirror nuclei in the fp shell. The measured GT strength represents only a small part of the total GT-strength value of 10.21 predicted by the shell-model calculation. However, since β^+ decay is sensitive only to the GT strength of the low-lying levels, it is impossible to draw any conclusion regarding the integrated GT strength. The calculated $B(\mathrm{GT})$ value for the ground-state transition is in good agreement with the experimental result. The shell-model calculations yield the ^{61}Ga half-life of 139 ms, again in good agreement with the experiment.

The measurement of the magnetic moments of the ^{61}Ga-^{61}Zn mirror pair is not feasible at present. Such a measurement would allow an estimation of the renormalized axial-vector constant [2]. On the another hand, accurate knowledge of logft in a mirror decay allows for a prediction of the magnetic moments. In Ref. [43] the authors derived the relation between the magnetic moments and logft based on an analysis of 18 well-studied mirror decays. Using the relations from [43] we obtain the predictions for the magnetic moments of $2.23(11)\mu_N$ and $-0.57(9)\mu_N$ for ^{61}Ga and ^{61}Zn, respectively. The magnetic moments obtained in the shell-model calculations are $1.96\mu_N$ and $-0.34\mu_N$ using the effective gyromagnetic factors $g^s = 0.75 g^s_{\mathrm{bare}}$, $g^l_\pi = 1.1\mu_N$, and $g^l_\nu = -0.1\mu_N$ and $2.31\mu_N$ and $-0.50\mu_N$ using bare gyromagnetic factors.

In conclusion, the β^+ decay of ^{61}Ga to the mirror nucleus ^{61}Zn has been studied. Pure Ga beams allowed for an accurate determination of the half-life, Q_{EC} value, and GT strength to low-lying transitions. The obtained results are consistent with the systematic trend for mirror decays in the fp shell. Further experimental and theoretical efforts are needed for extraction of the renormalized axial-vector constant.

ACKNOWLEDGMENTS

We would like to acknowledge the ISOLDE technical group for assistance during the experiment. We are also grateful to A. Folley, K. Van del Val, and Professor M. Huyse for help in the production of the β detectors, K. Salomaki for help in the design of the tape system, and T. Kalliokoski for help in preparing the software for the β-spectra analysis.

[1] S. Raman, C.A. Houser, T.A. Walkiewich, and I.S. Towner, At. Data Nucl. Data Tables **21**, 567 (1978).
[2] D.H. Wilkinson, Phys. Rev. C **7**, 930 (1973).
[3] J.F.A. Van Hienen, W. Chung, and B.H. Wildenthal, Nucl. Phys. **A269**, 159 (1976).
[4] E. Caurier, K. Langanke, G. Martinez-Pinedo, and F. Nowacki, Nucl. Phys. **A653**, 439 (1999) and references therein.
[5] H. Wilson, R.W. Kavanagh, and F.M. Mann, Phys. Rev. C **22**, 1696 (1980).
[6] J. Honkanen, V. Koponen, H. Hyvönen, P. Taskinen, J. Äystö, and K. Ogawa, Nucl. Phys. **A471**, 489 (1987).
[7] P. Hornshøj, J. Kolind, and N. Rud, Phys. Lett. **116B**, 4 (1982).
[8] T.W. Burrows, J.W. Olness, and D.E. Alburger, Phys. Rev. C **31**, 1490 (1985).

[9] J. Honkanen, V. Koponen, P. Taskinen, J. Äystö, K. Eskola, S. Messelt, and K. Ogawa, Nucl. Phys. **A496**, 462 (1989).
[10] J. Äystö, J. Ärje, V. Koponen, T. Taskinen, H. Hyvönen, A. Hautojárvi, and K. Vierinen, Phys. Lett. **138B**, 369 (1984).
[11] I. Reusen *et al.*, Phys. Rev. C **59**, 2416 (1999).
[12] D.R. Semon *et al.*, Phys. Rev. C **53**, R2602 (1996).
[13] J. Honkanen, M. Kortelahti, K. Eskola, and K. Vierinen, Nucl. Phys. **A366**, 109 (1981).
[14] M. Oinonen *et al.*, Eur. Phys. J. A **5**, 151 (1999).
[15] P. Baumann *et al.*, Phys. Rev. C **50**, 1180 (1994).
[16] M. Oinonen *et al.*, Phys. Rev. C **56**, 745 (1997).
[17] C.W. Woods, N. Stein, and J.W. Sunier, Phys. Rev. C **17**, 66 (1978).
[18] D.J. Weber, G.M. Crawley, W. Benenson, E. Kashy, and H. Nann, Nucl. Phys. **A313**, 385 (1979).
[19] P.J. Smith, L.P. Ekström, F. Kearns, P.J. Twin, and N.J. Ward, J. Phys. G **8**, 281 (1982)
[20] J.M. Thirion, G. Chouraqui, Th. Muller, and M. Port, Z. Phys. A **317**, 329 (1984).
[21] R.B. Schubank, J.A. Cameron, and V.P. Janzen, Phys. Rev. C **40**, 2310 (1989).
[22] S.M. Vincent *et al.*, Phys. Rev. C **60**, 064308 (1999).
[23] J.A. Winger *et al.*, Phys. Rev. C **48**, 3097 (1993).
[24] V.I. Mishin, V.N. Fedoseyev, H.-J. Kluge, V.S. Letokhov, H.L. Ravn, F. Scheerer, Y. Shirakabe, S. Sundell, O. Tengblad, and the ISOLDE Collaboration, Nucl. Instrum. Methods Phys. Res. B **73**, 550 (1993).
[25] V.N. Fedoseyev, G. Huber, U. Köster, J. Lettry, V.I. Mishin, H.L. Ravn, V. Sebastian, and the ISOLDE Collaboration, Hyperfine Interact. **127**, 409 (2000).
[26] A.N. Zherikhin, V.S. Letokhov, V.I. Mishin, M.E. Muchnik, and V.N. Fedoseyev, Appl. Phys. B: Photophys. Laser Chem. **6**, 47 (1983).
[27] L. Weissman *et al.*, Nucl. Instrum. Methods Phys. Res. A **423**, 328 (1999).
[28] C.N. Davis, C.A. Gagliardi, M.J. Murphy, and E.B. Norman, Phys. Rev. C **19**, 1463 (1979).
[29] E. Der Mateosian and A.W. Sunyar, At. Data Nucl. Data Tables **13**, 407 (1974).
[30] G. Audi *et al.*, Nucl. Phys. **A624**, 1 (1997).
[31] Jänecke and P.J. Masson, At. Data Nucl. Data Tables **39**, 265 (1988).
[32] W.E. Ormand, Phys. Rev. C **55**, 2407 (1997).
[33] P. Möller, J.R. Nix, W.D. Myers, and W.J. Swiatecki, At. Data Nucl. Data Tables **59**, 185 (1995).
[34] J.C. Hardy and I.S. Towner, Proceedings of ENAM98 Conference, Bellaire, Michigan, 1998, and references therein.
[35] N.B. Gove and M.J. Martin, Nucl. Data Tables **11**, 127 (1972).
[36] D.H. Wilkinson and B.E.F. Macefield, Nucl. Phys. **A232**, 58 (1974).
[37] E. Caurier, computer code ANTOINE, IReS, Strasbourg, 1989.
[38] A. Poves, J. Sánchez-Solano, E. Caurier, and F. Nowacki, Nucl. Phys. **A694**, 157 (2001).
[39] Particle Data Group, D.E. Groom *et al.*, Eur. Phys. J. C **15**, 1 (2000).
[40] G. Martinez-Pinedo, A. Poves, E. Caurier, and A.P. Zuker, Phys. Rev. C **53**, R2602 (1996).
[41] H. Schatz *et al.*, Phys. Rev. Lett. **86**, 3471 (2001).
[42] C. Mazzocchi *et al.*, Eur. Phys. J. (submitted).
[43] B. Buck, A.C. Merchant, and S.M. Perez, Phys. Rev. C **63**, 037301 (2000).